Chinese Chemical Letters 31 (2020) 2447–2451

Contents lists available at ScienceDirect

Chinese Chemical Letters

journal homepage: www.elsevier.com/locate/cclet

Communication

Rapid and fine tailoring longitudinal surface plasmon resonances of gold nanorods by end-selective oxidation

Wenhan Li[1], Zhirui Guo[1], Qiuyuan Tai, Yawen Li, Yefei Zhu*, Tingting Bai*

The Second Affiliated Hospital, Nanjing Medical University, Nanjing 210011, China

ARTICLE INFO

Article history:
Received 24 March 2020
Received in revised form 12 May 2020
Accepted 14 May 2020
Available online 18 May 2020

Keywords:
Gold nanorods
End-selective oxidation
$AuBr_4$-CTA complex
Longitudinal surface plasmon resonance

ABSTRACT

Facile achievement of gold nanorods (AuNRs) with controllable longitudinal surface plasmon resonance (LSPR) is of great importance for their applications in various fields. The LSPR of AuNRs is sensitive to their aspect ratio, which is still hard to be precisely tuned by direct synthesis. In this work, we report a simple approach for end-selective etching of AuNRs by a rapid oxidation process with Au(III) in cetyltrimethylammonium bromide (CTAB) solution at a mild temperature. The LSPR wavelength and the length of AuNRs blue shifted linearly as a function of the amount of Au(III), while the diameter of AuNRs remained nearly constant. The oxidative rate is temperature dependent, and the oxidative process for a desired LSPR can be accomplished within 15 min at 60 °C. Further investigations indicated that Br^- determine the occurrence of the oxidation between AuNRs and Au(III), and a small amount of surfactant chain (CTA^+) is crucial for stabilizing AuNRs. This method presents a quick but robust strategy for acquiring AuNRs with an arbitrary intermediate LSPR wavelength using the same starting AuNRs, and can be a powerful tool for subsequent applications.

Gold nanoparticles with shape-dependent plasmonic properties have received intensive studies and numerous applications [1–7]. Among a mass of available morphologies, single-crystal gold nanorod (AuNR) is a classic example of anisotropic nanoparticles that is particularly well-suited for biomedical fields, mainly owing to its unique plasmonic performances [8–10]. The isotropic counterpart of AuNR, the gold nanosphere, presents a single surface plasmon resonance. However, the one-dimensional anisotropy of AuNR results in two distinct plasmon resonances: the longitudinal plasmon resonance (LSPR) along the long axis of the particles and the transverse plasmon resonance (TSPR) along the short axis. While the TSPR wavelength of AuNRs constantly stays around 510 nm, the LSPR wavelength is sensitive to their aspect ratio (AR, length/diameter) and tunable from the visible to the near infrared-region (NIR). The latter is well-known as the biologically transparent window: the absorption by physiological fluids and tissues (*e.g.*, hemoglobin and water) is minimal in the first NIR (650−950 nm) and the imaging resolution (signal-to-noise ratio) together with the tissues penetration depth is greatly improved in the second NIR (1000−1350 nm). Currently, the available laser excitation wavelengths of commercial near-infrared diode-laser sources are 808 nm, 980 nm and 1064 nm, respectively. To achieve efficient bioimaging or photothermal therapy, the LSPR wavelength of AuNRs needs to match the laser wavelength as far as possible. Therefore, it is crucial for achieving on-demand LSPR wavelengths of AuNRs before the subsequent applications.

Among various AuNRs synthesis methods published, the seed-mediated, surfactant (often cetyltrimethylammonium bromide, CTAB)-assisted method originated by Murphy, Nikoobakht and El-Sayed is the most common one by far [11,12]. In a routine procedure, 1.5 nm gold seeds stabilized with CTAB is added to an Au(I)-CTAB solution, which is reduced from Au(III) with ascorbic acid in the presence of silver nitrate. This seeding procedure provides colloidal single-crystal AuNRs with low AR (2–5) in high yield (> 95%) and uniformity. These AuNRs have turned out to be stabilized by a bilayer of CTAB [13]. In particular, the curved two ends of AuNRs exhibit a lower density of CTAB than the longitudinal sides, enabling a higher chemical activity [14]. During the past decade, some modifications have been made to this CTAB-assisted seeding growth process and have produced a higher aspect ratio AuNRs with LSPR wavelength greater than 1200 nm [15,16]. This kind of seeding procedure, however, is susceptible to small changes of the experimental parameters, such as growth temperature, surfactant composition, seed quality, and even stirring speed [14]. It is often the case that the reliability and reproducibility of AuNRs varied significantly from batch to batch even for the identical person and procedure, which greatly

* Corresponding authors.
E-mail addresses: zhuyf@njmu.edu.cn (Y. Zhu), baitingting@njmu.edu.cn (T. Bai).
[1] These authors contributed equally to this work.

https://doi.org/10.1016/j.cclet.2020.05.019

limited regulation of the LSPR wavelengths of AuNRs with high precision.

Numerous efforts have been made to address this issue upon post-treatments of the AuNRs. There are primarily three practical approaches for turning the AR of AuNRs. One is the thermal reshaping: The pre-synthesized AuNRs dispersions are continuously annealed in hot baths [17,18]. The LSPR wavelength shows an exponential decay function of the heating time at a given temperature. This heating process also promotes the side growth leading to the "rounded" trend of AuNRs. The second is the overgrowth method: The AR of AuNRs is tailored by selectively expanding their diameters. As proposed by Wang group [19], small thiol molecules, such as glutathione or cysteine, are preferably bonded to the highly active ends of preformed AuNRs before the overgrowth, which hinders the longitudinal growth. As a result, AuNRs undergo a new round of transverse overgrowth, producing AuNRs with larger diameters but remaining lengths nearly unchanged. The third is the anisotropic oxidation: The length of AuNRs can be selectively shortened using proper oxidants at room temperature by virtue of the high reactivity of the ends [20–23]. As a consequence, the AR of AuNRs can be synthetically tuned over a wide range while keeping their diameters constant. However, existing anisotropic oxidation methods are usually time-consuming and prompt centrifugation is needed to prevent the desired AuNRs from further shortening.

Herein, we present a rapid and robust method for selectively shortening AuNRs with $AuBr_4$-CTA complex oxidation under mild temperature. This method allows for achieving AuNRs with any desired aspect ratio but a constant width from the same starting AuNRs through a 15 min oxidation process, and has no need of extra separation procedure. Typically, the synthesis of starting AuNRs was based on a routine CTAB-assisted seed-mediated method (Supporting information) [24]. The as-synthesized AuNRs dispersion was centrifuged and redispersed in 0.1 mol/L CTAB solution. For each sample, 10 mL of AuNRs with an optical density of 1.8 was mixed with a certain amount of 10 mmol/L $HAuCl_4$ and then maintained at 60 °C for 15 min. UV–vis-NIR extinction spectra were monitored and transmission electron microscopy (TEM) images were taken on AuNR samples obtained after oxidation.

Fig. 1A shows the extinction spectra recorded under different feeding amounts of Au(III). Starting AuNRs exhibited two extinction peaks, which were assigned to the TSPR and LSPR. The LSPR peak blue-shifted and decreased in intensity with the increasing the amount of Au(III), while the TSPR stayed at 508 nm and decreased slightly in intensity. Correspondingly, the AuNRs dispersion color changed from original brown to gray, cyan and blue in turn (Fig. 1A inset). Representative TEM images of AuNRs before and after oxidation are presented in Figs. 1B-E. The starting AuNRs exhibited a monodisperse size distribution with negligible shape impurities. Statistical analysis (Table S1 in Supporting information) shows these AuNRs had an average diameter of 19 ± 1.5 nm, an average length of 89 ± 6 nm, and an average AR of 4.6 ± 0.3. As shown in Figs. 1C-E, the length of AuNRs decreased with the increase of Au(III) volume, and the diameter hardly changed, revealing that the oxidation proceeded at the ends of the AuNRs.

To investigate the relationships among the LSPR shift and size change of AuNRs towards the Au(III) amount added, statistical analysis of at least 100 AuNRs at each stage was implemented from TEM images (Table S1). As shown in Fig. 2A, the blue-shift of the LSPR wavelength exhibited a nearly linear dependence on the Au(III) amount. Similarly, the length of AuNRs decreased steadily as a function of the Au(III) amount through the oxidation process, while the diameter remained nearly constant (Fig. 2B). Distinct from thermal reshaping methods, in which AuNRs exhibits a 'rounded' trend during the annealing process, the shortening of the AuNRs length did not cause the inevitable increase in diameter. Figs. 2C-E present the plots of the LSPR wavelength *versus* the size (length and diameter), aspect ratio and extinction of LSPR peak. These linear relationship results strongly suggested that our method could rapidly tailor the length of AuNRs to acquire various desired LSPR wavelength by changing the volume ratio between the Au(III) solution and original AuNRs dispersion.

Except for the Au(III) amount, there are two other factors involved in our method: reaction temperature and CTAB. To dig

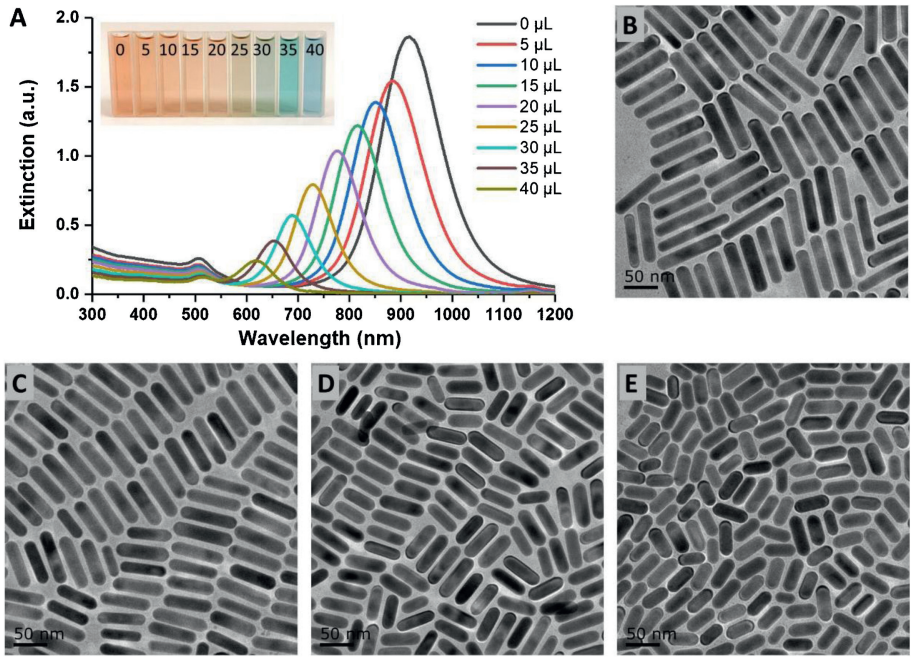

Fig. 1. (A) UV–vis spectra of AuNRs before and after oxidation with different volume 10 mmol/L $HAuCl_4$ solution in the presence of 0.1 mol/L CTAB. Inset shows the corresponding photographs of the solutions. TEM images of (B) as-synthesized AuNRs and shortened AuNRs after the addition of (C)15 μL, (D) 25 μL and (E) 35 μL of 10 mmol/L $HAuCl_4$ solution.

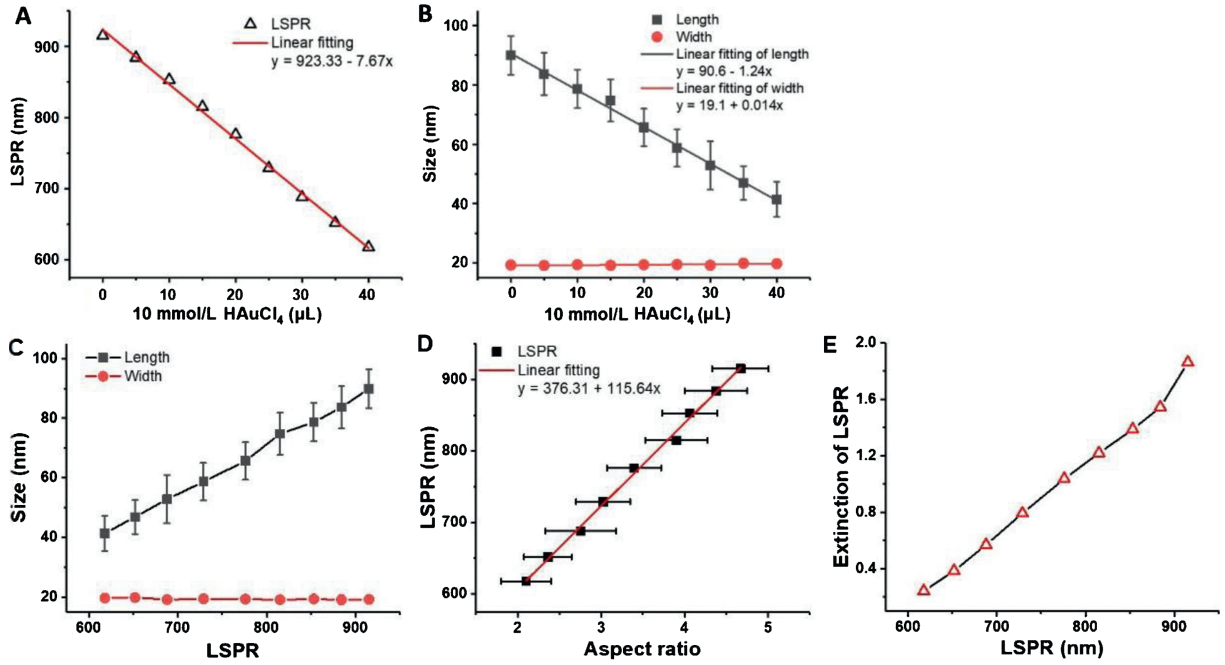

Fig. 2. (A) LSPR peak and (B) size changes of the shortened AuNRs as a function of $HAuCl_4$ volume. (C) Size changes *versus* the LSPR wavelength of the shortened AuNRs. (D) LSPR wavelength *versus* the aspect ratio of the shortened AuNRs. (E) Peak extinction values extracted from Fig. 1A *versus* the LSPR wavelength.

deeply into the influence of these factors on the oxidation of AuNRs and get a better understanding of the inner mechanism, several pragmatic controlled trials were further conducted. In a set of experiments, the same AuNRs solutions were oxidized at different temperatures from 30 °C to 70 °C with an interval of 10 degrees. As shown in Fig. 3, the oxidation drastically took place on the AuNRs in the first five minutes as evidenced by the large blue-shift for all the given temperatures. Then, the blue-shift tended to slow down with the elapse of reaction time, which is attributed to the gradual consumption of Au(III). It clearly stated that the blue-shift of LSPR was quite sensitive to the reaction temperature. At the typical temperature of 60 °C, the LSPR peak of the AuNRs colloidal solution rapidly blue shifted from 915 nm to 816 nm after the addition of 15 μL of 10 mmol/L $HAuCl_4$ solution within 15 min, which is the end point of this reaction. The same situation showed up at the temperature of 70 °C. However, the LSPR peak had smaller blue-shift rates at lower temperatures within the same reaction time. Oxidation of AuNRs at 30 °C normally took a few good hours to consume the entire amount of Au(III). Therefore, a mild temperature of 60 °C was applied as the optimal reaction temperature, which takes the reaction efficiency into account and avoids the thermal reshaping effect of higher temperature.

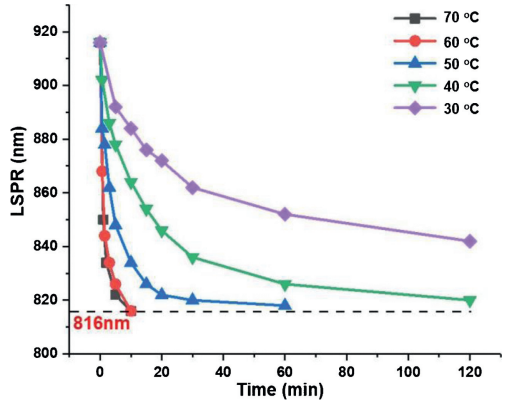

Fig. 3. The LSPR wavelength of AuNRs is ploted as a function reaction time at different reaction temperature. The solution was a mixture of 10 mL as-synthesized AuNRs solution in 0.1 mol/L CTAB and 15 μL of 10 mmol/L $HAuCl_4$.

It has documented that the oxidation mechanism of Au nanoparticles using Au(III) as the oxidant is a conproportionation reaction in nature, which cannot occur without CTAB since the resultant $AuCl_2^-$ is highly unstable in this situation (Eq. 1) [25]. When CTAB stabilized Au nanoparticles are mixed with Au(III) such as $AuCl_4^-$, the ligand exchange from $AuCl_4^-$ to $AuBr_4^-$ will occur and lead to the following formation of $AuBr_4$-CTA complex, which influences their redox potentials and pushes the equilibrium toward the conproportionation reaction between Au(III) and Au(0) (Eqs. 2 and 3). Meanwhile, the final resultant in the form of $AuBr_2$-CTA complex is highly stable. Therefore, AuNRs is shortened in this scenario.

$$AuCl_4^- + 2Au = 3AuCl_2^- \quad \text{(highly unstable)} \tag{1}$$

$$AuCl_4^- \leftrightarrow AuCl_3Br^- \leftrightarrow AuCl_2Br_2^- \leftrightarrow AuClBr_3^- \leftrightarrow AuBr_4^- \tag{2}$$

$$AuBr_4 - CTA + 2AU + 2CTA^+ + 2BR^- = 3AuBr_2 - CTA \tag{3}$$

It could be indicated by Eq. 3 that the concentration increase of CTAB is favorable for the oxidation of AuNRs. Our control experiments further confirmed that the oxidative rate of AuNRs rose with the concentration increase of CTAB (Fig. 4A). Moreover, it was observed that the oxidation process was still on even when the CTAB concentration was heavily reduced to 5 mmol/L. In another control trial, AuNRs were washed and resuspended in CTAC solution under the same concentration (5 mmol/L), no changes in the LSPR peak were observed during the detection time (Fig. 4A), which indicates that Br^- plays an important role in the occurrence of this oxidation reaction. Besides, the effect of CTA^+ on the oxidation of AuNRs was also investigated by replacing CTAB with the same concentration of bromide (0.1 mol/L NaBr) in the presence of 0.5 mmol/L CTAC, which is important and sufficient to stabilize the AuNRs from aggregation. During the reaction time,

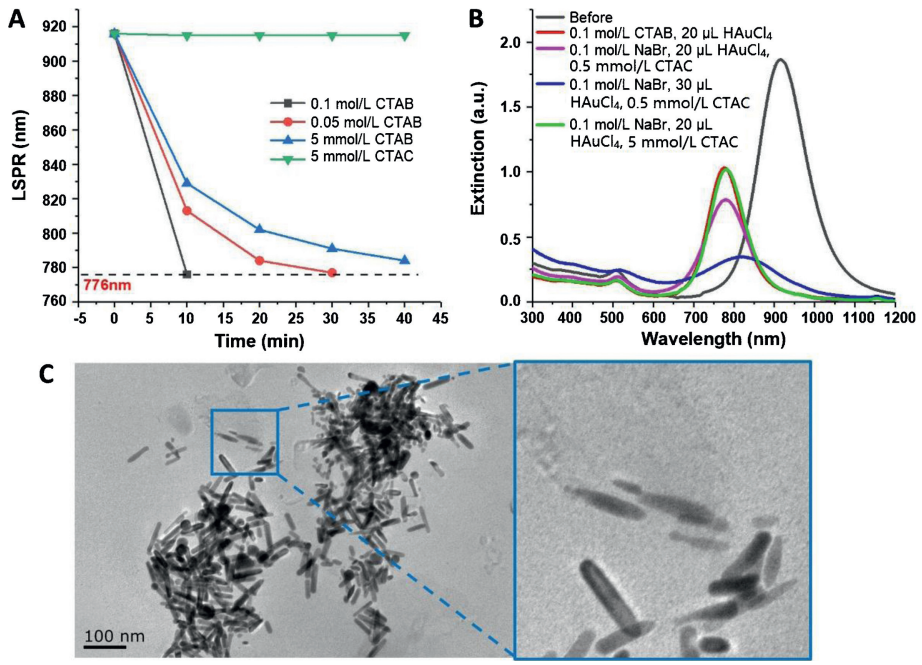

Fig. 4. (A) The LSPR wavelength of shortened AuNRs is ploted as a function reaction time under different concentrations of surfactant (CTAB and CTAC). The solution was a mixture of 10 mL as-synthesized AuNRs solution and 20 μL of 10 mmol/L $HAuCl_4$. (B) UV–vis spectra of shortened AuNRs acquired under the same concentration of Br^- (0.1 mol/L), but different concentration of CTA^+ surfactant. (C) TEM image of shortened AuNRs. 10 mL as-synthesized AuNRs solution in 0.1 mol/L NaBr and 0.5 mmol/L CTAC was mixture with 20 μL of 10 mmol/L $HAuCl_4$.

the shape of LSPR peak greatly broadened and the intensity of TSPR peak increased after adding $HAuCl_4$ solution (Fig. 4B). These spectra changes indicated that the oxidation of AuNRs took place over the whole surface, which was supported by TEM observation (Fig. 4C). When the concentration of CTAC was increased only to 5 mmol/L, the oxidation process of AuNRs in the presence of 0.1 mol/L NaBr was nearly the same as that in 0.1 mol/L CTAB. Thus, it is suggested that, if the concentration of CTA^+ is assured to cover the surface of AuNRs, the occurrence and efficiency of AuNRs oxidation in our method are mainly determined by Br^-. Moreover, NaBr can be a beneficial substitute in shortening AuNRs from an environmental point of view, since CTAB has a higher biological toxicity [26,27].

Finally, the generality of this method on shortening AuNRs was investigated since a number of improved methods of synthesizing AuNRs have emerged in recent years. Two different AuNRs were chosen and oxidized by our method. They were synthesized by a binary surfactant (CTAB and NaOL)-assisted seeding method and a CTAB-assisted seeding method with hydroquinone as the reductant. As shown in Fig. 5, these two kinds of AuNRs had a LSPR peak at 1150 nm and 1192 nm respectively. By means of the end-selective etching method developed in this study, AuNRs with four typical LSPR peaks (785 nm, 808 nm, 980 nm and 1064 nm) were all easily achieved from these two kinds of AuNRs.

In summary, a rapid end-selective shortening of AuNRs by the oxidation of $AuBr_4$-CTA complexes has been carried out to prepare AuNRs with tunable LSPR wavelength from the same starting AuNRs at a mild temperature. Our results demonstrated that, the oxidation rate is temperature dependent, and the etching process can be finished within 15 min at 60 °C. The diameter of AuNRs remained nearly constant during shortening, while the length of AuNRs decreased linearly as the function of the feeding Au(III) amount. Moreover, it was evidenced that Br^- activated the oxidation between AuNRs and Au(III). Thus, the shortening of AuNRs can be equally achieved by NaBr instead of concentrated CTAB. By precisely calculating the addition of $HAuCl_4$ solution, this method enables the synthesis of AuNRs with any desired intermediate LSPR wavelength. We believe that this simple and straightforward method will lay a solid foundation for AuNRs in a variety of optical and biomedical applications.

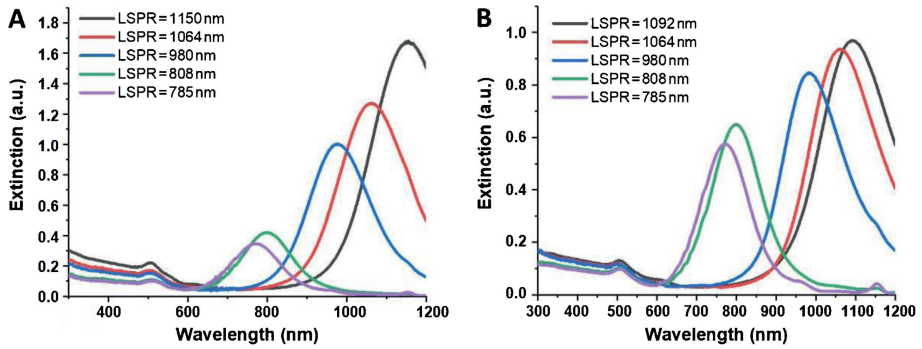

Fig. 5. UV–vis spectra of shortened AuNRs with four typical LSPR peaks (785 nm, 808 nm, 980 nm and 1064 nm) acquired from two kinds of AuNRs: (A) NaOL and (B) hydroquinone-mediated synthetic method.

Declaration of competing interest

The authors declare that they have no known competing financial interests or personal relationships that could have appeared to influence the work reported in this paper.

Acknowledgments

This work is financially supported by the National Natural Science foundation of China (No. 81701849) and Science and Technology Support Project of Jiangsu Province (No. BE2017763).

Appendix A. Supplementary data

Supplementary material related to this article can be found, in the online version, at doi:https://doi.org/10.1016/j.cclet.2020.05.019.

References

[1] D. Zhang, S. Du, S. Su, et al., Biosens. Bioelectron. 123 (2019) 19–24.
[2] J.J. Shen, P.H. Zhang, F. Zheng, et al., ACS Appl. Nano Mater. 1 (2018) 2120–2128.
[3] T. Li, J. Sun, J. Liu, et al., Chin. Chem. Lett. 31 (2020) 439–442.
[4] Z. Zhang, L.M. Bragg, M.R. Servos, et al., Chin. Chem. Lett. 30 (2019) 1655–1658.
[5] J. Song, L. Wang, H. Qi, et al., Chin. Chem. Lett. 30 (2019) 1643–1646.
[6] S. Zeng, H. Yuan, L. Gan, et al., Chin. Chem. Lett. 30 (2019) 1266–1268.
[7] C. Shang, C. Cai, C. Zhao, et al., Chin. Chem. Lett. 29 (2018) 81–83.
[8] K. Zhang, T. Bai, M. Wang, et al., Nanosci. Nanotechnol. Lett. 10 (2018) 119–126.
[9] D. Yuan, H. Yan, J. Liu, et al., Chin. Chem. Lett. 31 (2020) 455–458.
[10] L. Zhang, H. Su, J. Cai, et al., ACS Nano 10 (2016) 10404–10417.
[11] N.R. Jana, L. Gearheart, C.J. Murphy, J. Phys. Chem. B 105 (2001) 4065–4067.
[12] B. Nikoobakht, M.A. El-Sayed, Chem. Mater. 15 (2003) 1957–1962.
[13] B. Nikoobakht, M.A. El-Sayed, Langmuir 17 (2001) 6368–6374.
[14] H. Chen, L. Shao, Q. Li, et al., Chem. Soc. Rev. 42 (2013) 2679–2724.
[15] X. Ye, Y. Gao, J. Chen, et al., Nano Lett. 13 (2013) 2163–2171.
[16] L. Vigderman, E.R. Zubarev, Chem. Mater. 25 (2013) 1450–1457.
[17] L. Gou, C.J. Murphy, Chem. Mater. 17 (2005) 3668–3672.
[18] K.C. Ng, W. Cheng, Nanotechnology 23 (2012) 105602.
[19] W. Ni, X. Kou, Z. Yang, et al., ACS Nano 2 (2008) 677–686.
[20] J. Rodríguez-Fernández, J. Pérez-Juste, P. Mulvaney, et al., J. Phys. Chem. B 109 (2005) 14257–14261.
[21] C.K. Tsung, X. Kou, Q. Shi, et al., J. Am. Chem. Soc. 128 (2006) 5352–5353.
[22] R. Zou, X. Guo, J. Yang, et al., CrystEngComm 11 (2009) 2797–2803.
[23] B. Zhang, Y. Xia, Chin. Chem. Lett. 30 (2019) 1663–1666.
[24] H. Chen, X. Kou, Z. Yang, et al., Langmuir 24 (2008) 5233–5237.
[25] T. Bai, Y. Tan, J. Zou, et al., J. Phys. Chem. C 119 (2015) 28597–28604.
[26] L. Wang, X. Jiang, Y. Ji, et al., Nanoscale 5 (2013) 8384–8391.
[27] P. Wang, X. Wang, L. Wang, et al., Sci. Technol. Adv. Mater. 16 (2015) 034610.